

Tuning Excess Noise by Aharonov-Bohm Interferometry

Fabrizio Dolcini^{1,*} and Hermann Grabert^{2,3}

¹*Dipartimento di Fisica del Politecnico di Torino, I-10129 Torino, Italy*

²*Physikalisches Institut, Albert-Ludwigs-Universität, 79104 Freiburg, Germany*

³*Freiburg Institute for Advanced Studies (FRIAS),
Albert-Ludwigs-Universität, 79104 Freiburg, Germany*

A voltage bias applied to a conductor induces a change of the current noise with respect to the equilibrium noise known as excess noise. We analyze the excess noise of the electronic current flowing through a mesoscopic Aharonov-Bohm ring threaded by a magnetic flux, coupled to a side gate, and contacted by two metallic electrodes. It is shown that the excess noise can be controlled both magnetically and electrostatically, demonstrating the full tunability of the system. At zero frequency, the ratio of the noise strength to the current (Fano factor) can thereby be minimized. Remarkably, at finite frequency, regions of negative excess noise emerge.

I. INTRODUCTION

Electronic conduction is an important phenomenon arising in a broad variety of systems in different fields, ranging from physics to engineering and chemistry. Conductors can be organic and inorganic materials, and there are bulk materials like metals, molecular systems such as polymers or DNA, as well as micro-fabricated devices. The most important property of a conductor is its current-voltage characteristics, i.e. the dependence of the current on the applied voltage bias. Just like any observable, the current also exhibits fluctuations around its average value, usually referred to as *noise*. As this term suggests, noise was originally regarded to as a disturbing feature, possibly jeopardizing the stability of the signal in an electronic circuit. In recent years, however, especially in the field of mesoscopic physics, Rolf Landauer's famous remark that noise can be regarded as a signal too, has been substantiated by demonstrating that current noise contains remarkably useful information about the conductor.¹⁻³ For fractional quantum Hall systems, for instance, it has been shown that noise measurements allow to observe the quasiparticle fractional charge characterizing the edge channels^{4,5}. More recently, in the field of nanoelectromechanical systems (NEMS) it has been realized that, under appropriate conditions, noise can even be exploited to cool a mechanical resonator^{6,7}.

The current noise at a measurement position x and at a frequency ω is defined as

$$S^+(\omega, V; x) = \int_{-\infty}^{+\infty} dt e^{i\omega t} \langle \Delta \hat{J}(x, t) \Delta \hat{J}(x, 0) \rangle \quad (1)$$

where $\Delta \hat{J}(x, t) = \hat{J}(x, t) - \langle \hat{J} \rangle$ is the current fluctuation operator, and V is the bias voltage applied to the conductor. Eq. (1) represents the non-symmetrized version of the noise, which has recently attracted attention in mesoscopic physics, for it can be directly measured by on-chip detectors⁸⁻¹⁰.

At equilibrium ($V = 0$) the average current through a conductor vanishes. Nevertheless, noise may be present because of thermal fluctuations (arising at finite temperature) and quantum fluctuations (arising at finite frequency)¹¹. While the role of thermal noise (also known as Johnson-Nyquist noise) has been investigated since long^{12,13}, the regime $\hbar\omega > k_B T$, where quantum mechanics plays an important role, has become accessible only more recently thanks to advances in the design of high frequency electronics operating at low temperatures^{14,15}.

We shall focus here on the purely quantum-mechanical regime, and consider henceforth the case of zero temperature. Quantum fluctuations become manifest in a non-vanishing absorption noise spectrum of the conductor, i.e. $S^+(\omega, 0; x) \neq 0$ for $\omega > 0$, and originate from processes where electrons absorb an energy quantum $\hbar\omega$ from the environment, typically a spectrum detector coupled to the conductor¹⁶. When the system is driven out of equilibrium by an applied voltage bias V , an additional source of noise arises, due to the quantization of the electronic charge leading to a partitioning of electron scattering¹⁷⁻²⁰.

On the experimental level, current and noise measurements are usually performed with an amplifier, which in turn exhibits its own intrinsic noise, often higher than the noise of the conductor to be measured. In order to avoid this problem and improve the signal-to-noise ratio, it is favorable to measure the excess noise, i.e. the difference between the noise in presence of a finite bias voltage V and the equilibrium noise

$$S_{\text{EX}}(\omega, V; x) \doteq S^+(\omega, V; x) - S^+(\omega, 0; x). \quad (2)$$

The excess noise can also be expressed as

$$S_{\text{EX}}(\omega, V; x) = \int_0^V \frac{\partial S^+(\omega, V'; x)}{\partial V'} dV'. \quad (3)$$

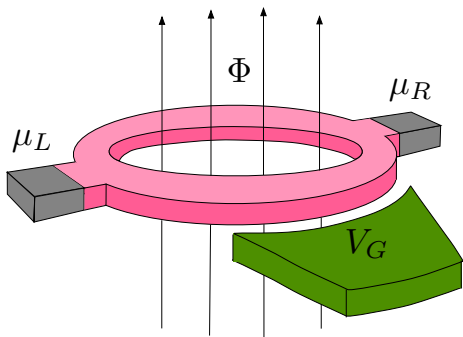


FIG. 1. Sketch of the Aharonov-Bohm interferometer. A ring threaded by a magnetic flux Φ is connected to two metallic electrodes at electrochemical potentials μ_L and μ_R implying a voltage bias $V = (\mu_L - \mu_R)/e$. A side gate with gate voltage V_G is coupled to one of the two arms of the interferometer.

In view of the additional noise generating processes arising in presence of a finite voltage V , excess noise is usually expected to be a positive quantity. This intuition is, however, wrong in general. Indeed Lesovik and Loosen²¹ have pointed out that in the regime $eV \gg k_B T$ the shot noise $S^+(0, V; x)$ becomes smaller than the equilibrium Johnson-Nyquist noise when the transmission coefficient of a conductor is non-vanishing only in an energy window δE , the Fermi energy lies within this energy window, and the temperature is sufficiently high ($k_B T \gg \delta E$). More recently, it has been shown that the excess noise can be negative also in the quantum regime²², implying the formation of an out of equilibrium state with noise smaller than the equilibrium quantum noise.

To clarify the conditions leading to negativity of the excess noise, it is natural to inquire whether the noise measured at a given applied voltage bias V can be tuned. One possibility to tune the noise is to change the number of conducting channels by applying a gate voltage to the conductor, as is routinely done, for instance, with quantum point contacts²⁰. This requires a multi-channel conductor and induces nearly discrete changes. In contrast, here we look for lines in the parameter space separating regimes of different sign of the excess noise, so that continuous tuning would be desirable. To this purpose, a suitable system is a quantum interferometer. Indeed, interferometers offer the appealing feature that scattering properties can be tuned via the interference conditions, opening the possibility to modify the current noise while keeping the voltage V (and possibly also the frequency ω) fixed. In this paper, using a concrete model system, we shall show that excess noise can indeed be tuned to negative values.

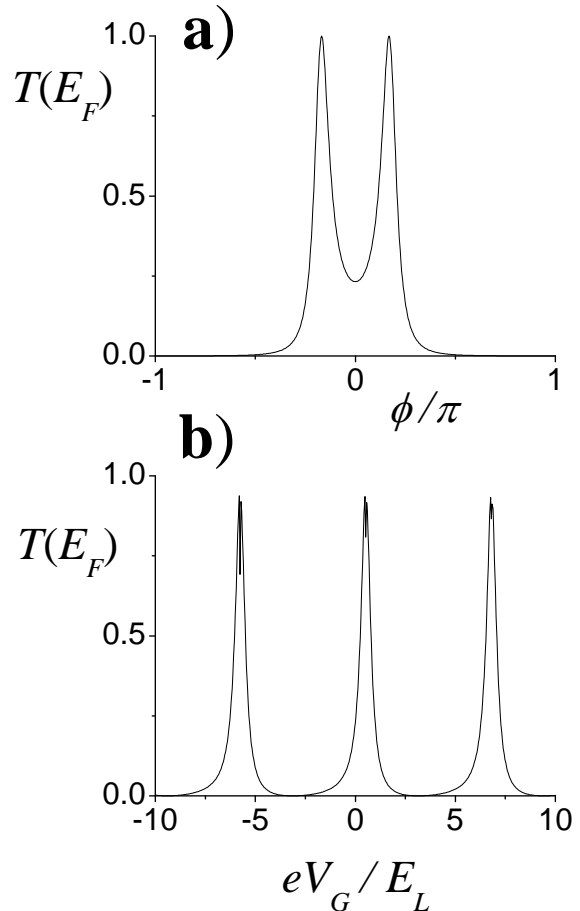


FIG. 2. The transmission coefficient of the Aharonov-Bohm ring at the Fermi energy $E_F = 100 E_L$ is plotted as a function of (a) the dimensionless magnetic flux ϕ and (b) the side gate voltage $u = eV_G/E_L$.

II. THE MODEL

In order to illustrate the effect of noise tuning, we shall consider an Aharonov-Bohm interferometer, consisting of a ring contacted by two electrodes, as depicted in Fig. 1. The ring is threaded by a magnetic flux Φ ; furthermore we envisage a side gate which changes the potential of the (say) lower arm with respect to the upper arm by an amount V_G . The interference condition between electron propagation in the two arms can therefore be controlled both magnetically, through the flux, and electrostatically, through the side gate voltage V_G . For simplicity we assume that the ring is symmetric and narrow so that the electrons propagate in a single channel. The contacts of the ring to the electrodes are modeled as Y-junctions, characterized by the customary scattering matrix^{23,24}

$$S_Y(\eta) = \begin{pmatrix} -\sqrt{1-2\eta} & \sqrt{\eta} & \sqrt{\eta} \\ \sqrt{\eta} & a(\eta) & b(\eta) \\ \sqrt{\eta} & b(\eta) & a(\eta) \end{pmatrix} \quad (4)$$

with $a(\eta) = (\sqrt{1-2\eta}-1)/2$ and $b(\eta) = (\sqrt{1-2\eta}+1)/2$. Here $\eta \in [0; 1/2]$ is a parameter interpolating between total reflection and perfect transmission of an electron approaching the Y-junction from the lead. Propagation of the electron wave function along the two arms of the ring involves phase factors that depend on the magnetic flux Φ , as well as on the side gate voltage V_G applied to the lower arm. For simplicity, we shall neglect here flux and side gate voltage fluctuations, which have been addressed elsewhere²⁵⁻²⁷.

Combining the scattering matrices (4) at the two contacts with the propagation along the arms, a rather lengthy but straightforward calculation yields the scattering matrix for the Aharonov-Bohm interferometer

$$S_E = \begin{pmatrix} r_E & t'_E \\ t_E & r'_E \end{pmatrix} \quad (5)$$

where E denotes the energy of the incident electron and r and r' (t and t') are the reflection (transmission) amplitudes. These matrix elements can be suitably expressed as²⁸ $r = r' = \rho_P/P^*$, $t = -i\tau_P^*/P^*$, and $t' = -i\tau_P/P^*$, with

$$P(\varepsilon) = \left[e^{i(\varepsilon + \kappa_F + \frac{\pi}{2})} - e^{-i(\varepsilon + \kappa_F + \frac{\pi}{2})} \cos \gamma \right]^2 + 4 \cos \gamma \sin^2 \left(\frac{\phi}{2} \right) - (1 - \cos \gamma)^2 \prod_{s=\pm} \cos \left(\frac{u + s\phi}{2} \right), \quad (6)$$

$$\tau_P(\varepsilon) = -i \sin^2 \gamma \prod_{s=\pm} s e^{i s (\varepsilon + \kappa_F + \frac{\pi}{2})} \times \cos \left(\frac{u + s\phi}{2} \right), \quad (7)$$

and

$$\rho_P(\varepsilon) = 4 \cos \gamma \prod_{s=\pm} \sin \left(\varepsilon + \kappa_F + \frac{u + s\phi}{2} \right) + (1 - \cos \gamma)^2 \prod_{s=\pm} \sin \left(\frac{u + s\phi}{2} \right). \quad (8)$$

Here $\varepsilon = (E - E_F)/E_L$ describes the deviation of the energy E from the Fermi level E_F , expressed in terms of the ring ballistic frequency

$$E_L = \hbar v_F / L, \quad (9)$$

where L is the length of either ring arm; $u = eV_G/E_L$ is the dimensionless side gate voltage, $\kappa_F = k_F L$ is

the dimensionless Fermi wavevector, and $\phi = 2\pi\Phi/\Phi_0$ is the dimensionless flux, with $\Phi_0 = h/e$ denoting the flux quantum. Finally, $\gamma \in [0; \pi/2]$ is a convenient re-parametrization of the Y-junction transparency $T_Y = \sin^2 \gamma$ which is related with η in Eq. (4) through the relation $\eta = (\sin^2 \gamma)/2$. The spectrum of the ring has been linearized around the equilibrium Fermi energy E_F , under the realistic assumption that all relevant electronic energies deviate from the Fermi energy by an energy difference much smaller than E_F . We note in passing that the presence of the magnetic flux ϕ makes the scattering matrix (5) non-symmetric due to the breaking of time-reversal symmetry.

The tunability of the Aharonov-Bohm interferometer is explicitly shown in Fig. 2, where the transmission coefficient $T_E = |t_E|^2 = |t'_E|^2$ of the ring at the Fermi energy E_F is shown as a function of the magnetic flux [see Fig. 2(a)] and the side gate voltage [see Fig. 2(b)]. The current operator at a measurement point located in the (say) left lead reads

$$\hat{J}(x, t) = \frac{e}{2\pi\hbar} \int_{-\infty}^{\infty} \int_{-\infty}^{\infty} dE dE' e^{i(E-E')t/\hbar} \times \sum_{X,Y=L/R} \left\{ A_L^{XY}(E, E'; x) : \hat{a}_{XE}^\dagger \hat{a}_{YE'} : \right\} \quad (10)$$

where the symbol $::$ denotes normal ordering with respect to the equilibrium Fermi sea, the label L [R] refers to the left [right] lead, and the dimensionless coefficients A_L^{XY} are related to the elements of the scattering matrix (5) by

$$\begin{aligned} A_L^{LL}(E, E'; x) &= e^{-i(k_E - k_{E'})x} - e^{i(k_E - k_{E'})x} r_E^* r_{E'} \\ A_L^{RR}(E, E'; x) &= -e^{i(k_E - k_{E'})x} t_E^* t_{E'} \\ A_L^{LR}(E, E'; x) &= -e^{i(k_E - k_{E'})x} r_E^* t_{E'} \\ A_L^{RL}(E, E'; x) &= -e^{i(k_E - k_{E'})x} t_E^* r_{E'}. \end{aligned} \quad (11)$$

Substituting this expression into the definition (1) of the non-symmetrized current noise at a measurement point x located in the (say) left electrode, one obtains

$$S^+(\omega, V; x) = \frac{e^2}{2\pi\hbar} \int_{-\infty}^{\infty} dE \sum_{X,Y=L,R} |A_L^{XY}(E, E + \hbar\omega; x)|^2 f_X(E)(1 - f_Y(E + \hbar\omega)), \quad (12)$$

where $f_{L/R}(E) = f(E - \mu_{L/R})$ denotes the Fermi distribution function in the L/R lead with the electrochemical potential $\mu_{L/R} = E_F + e a_{L/R} V$. Here

$$V = (\mu_L - \mu_R)/e \quad (13)$$

is the applied voltage, while a_L and $a_R = a_L - 1$ are numerical coefficients depending on the biasing scheme.

For symmetric bias $a_L = a_R = 1/2$ while for completely asymmetric bias one of the coefficients vanishes.

A straightforward calculation also yields the voltage derivative of the noise at zero temperature

$$\begin{aligned} \frac{\partial S^+}{\partial V}(\omega, V; x) &= \frac{e^3}{2\pi\hbar}. \quad (14) \\ \left\{ \theta(\omega) \sum_{X=L,R} a_X \sum_{s=\pm 1} s |A_L^{XX}(\mu_X, \mu_X + s\hbar\omega; x)|^2 \right. \\ &+ \theta(\hbar\omega + eV) \left[a_L |A_L^{LR}(\mu_L, \mu_L + \hbar\omega; x)|^2 \right. \\ &\quad \left. \left. - a_R |A_L^{LR}(\mu_R - \hbar\omega; \mu_R; x)|^2 \right] \right. \\ &\left. - \theta(\hbar\omega - eV) \left[a_L |A_L^{RL}(\mu_L - \hbar\omega; \mu_L; x)|^2 \right. \right. \\ &\quad \left. \left. - a_R |A_L^{RL}(\mu_R, \mu_R + \hbar\omega; x)|^2 \right] \right\} \end{aligned}$$

and the excess noise is easily computed from Eq. (3).

As one can see, the noise depends on the coefficients A_L^{XY} which are related to the scattering matrix of the mesoscopic system [see Eq. (11)]. In particular, we shall show below that, because of competing signs in front of the various terms in Eq. (14), the excess noise may be driven to negative values.

III. RESULTS AND DISCUSSION

A. Shot noise

We start our analysis with the case $\omega = 0$ (shot noise): at zero frequency (and zero temperature) the equilibrium noise vanishes and the excess noise coincides with the shot noise. Now, from Eqs. (11) and (12) we see that the shot noise

$$S_0^+(V) \equiv S^+(\omega = 0, V; x) \quad (15)$$

is independent of the measurement position x since the same is true for the coefficients $A_L^{XY}(E, E'; x)$ for $E = E'$. The Fano factor

$$F = \frac{S_0^+(V)}{eI} \quad (16)$$

quantifies the ratio of the noise to the average current. To illustrate the benefit of the Aharonov-Bohm interferometer, we first focus on the regime of small applied bias $eV \ll E_L \ll E_F$: In this case the transmission and reflection coefficients depend only very weakly on energy, and one recovers the well known expressions $I = (e^2/h)TV$ for the average current and $S_0^+ = (e^3/h)T(1-T)V$ for the shot noise. Exploiting the dependence of the transmission coefficient T on the magnetic flux and the side gate potential, it is thus possible to tune the transport conditions, for example, to a minimum of the Fano factor, as

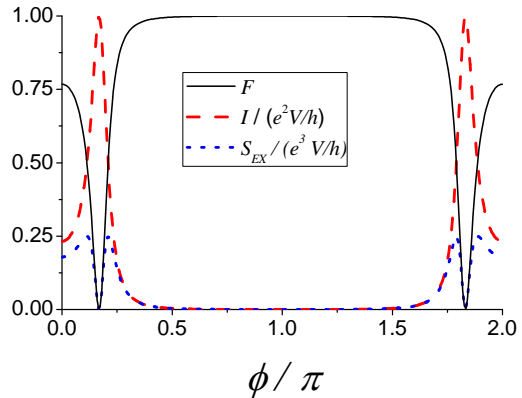


FIG. 3. The Fano factor (solid curve), the dimensionless current (dashed curve) and the shot noise (dotted curve) of an Aharonov-Bohm interferometer biased with a voltage $eV = E_L/100$ are plotted as a function of the dimensionless magnetic flux. The ring parameters are $\gamma = \pi/6$, $E_F = 100 E_L$, and $a_L = 1/2$.

shown in Fig. 3. Similar results have also been obtained within a tight-binding approach²⁹, and for the case of quantum dots embedded in the arms of an Aharonov-Bohm interferometer^{30,31}.

In general, if the applied voltage is comparable with (or bigger than) the ballistic ring energy E_L , the energy dependence must be taken into account and the noise is readily obtained from Eq. (3) upon integration of the expression

$$\begin{aligned} \frac{\partial S^+}{\partial V}(\omega = 0, V; x) &= \frac{e^3}{h} \text{sgn}(V) \quad (17) \\ &\times [a_L T(\mu_L)R(\mu_L) - a_R T(\mu_R)R(\mu_R)] \end{aligned}$$

which follows from Eq. (14) for $\omega = 0$.

B. Finite frequency noise

Let us now consider the case of finite frequency $\omega \neq 0$. Then the equilibrium noise $S^+(\omega; 0; x)$ is non-vanishing due to quantum fluctuations, so that the excess noise S_{EX} differs from the total current noise even at zero temperature. Crucial differences with respect to the zero frequency case emerge mainly in view of two important aspects. In the first instance, the energy dependence of the scattering matrix may become important even in the regime of very small voltage bias, if the frequency is comparable with the ring ballistic frequency E_L/\hbar . Secondly, finite frequency measurements are able to resolve the internal dynamics of the conductor and are thus sensitive to instantaneous charge fluctuations caused by current flow. These fluctuations induce instantaneous changes of the potential profile U inside the

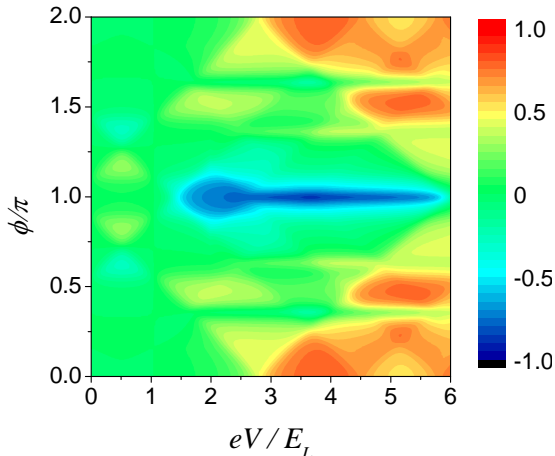


FIG. 4. The excess noise (in units of $e^2 E_L / h$) at finite frequency $\omega = 2E_L / \hbar$ is plotted as a function of the applied bias voltage V and the dimensionless magnetic flux $\phi = 2\pi\Phi/\Phi_0$. Regions of negative excess noise can be reached by magnetic tuning of the Aharonov-Bohm ring flux. The ring parameters are $\gamma = \pi/6$, $E_F = 100E_L$, $a_L = 1/2$, $V_G = 0$, and the measurement point is at the left contact.

conductor, which in turn affect the scattering properties. Because of this feed-back process, the determination of finite frequency transport properties is essentially an *interacting* problem^{32–34} for which the potential profile U must be determined self-consistently.

The above-mentioned factors affect the finite frequency noise in unlike ways, thus leading to rather rich finite frequency current noise features. A specific question we wish to address here is whether the out of equilibrium noise may become smaller than the equilibrium noise, thus leading to negative excess noise. The investigation of this problem is quite difficult in general, because various factors interplay, in particular, the energy dependence of the scattering matrix, the frequency regime under investigation, and the internal screening properties of the conductor. Some approximations are thus necessary in order to proceed. A simple but effective method to account for the instantaneous potential profile fluctuations ΔU in terms of a single parameter is based on the geometrical capacitance C relating the spectrum $\Delta U(\omega)$ of potential variations to the electronic charge spectrum $Q(\omega)$ through the relation $\Delta U(\omega) \sim Q(\omega)/C$. The importance of potential profile fluctuations thus strongly depends on the size of the geometrical capacitance C , which has to be compared with the intrinsic quantum capacitance C_q of the conductor, related to its density of states.

In a recent paper²² investigating the excess noise of a single channel quantum wire, we have shown that the

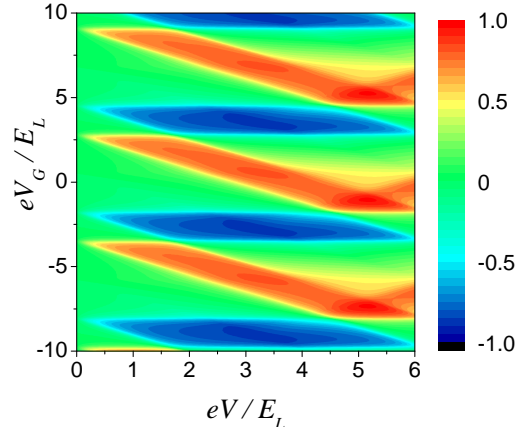


FIG. 5. The excess noise (in units of $e^2 E_L / h$) at finite frequency $\omega = 2E_L / \hbar$ is plotted as a function of the applied bias voltage V and the side gate voltage V_G . Regions of negative excess noise can be reached by electrostatic tuning of the side gate potential. The ring parameters are $\gamma = \pi/6$, $E_F = 100E_L$, $a_L = 1/2$, $\phi = 0$, and the measurement point is at the left contact.

excess noise becomes negative when the geometrical capacitance is smaller than $1/3$ of the quantum capacitance. Here, instead, we shall focus on the case of a large geometrical capacitance $C \gg C_q$, when fluctuations of the charge of the ring induce negligible variations in the potential U , so that the independent electron approach remains valid. Nevertheless, since transport is analyzed at finite frequency, the energy dependence of the scattering matrix is important³⁵. Indeed, the noise $S^+(\omega, V; x)$, which is always positive, can be expressed as an integral of scattering matrix elements $|A_L^{XY}|^2$ over energy windows determined by the Fermi functions of the leads [see Eq.(12)]. Importantly, the out of equilibrium noise and the equilibrium quantum noise are characterized by different energy windows, because the former depend on the applied voltage V , besides the finite frequency ω . By varying the energy profile of the scattering matrix via Aharonov-Bohm interferometry, the out of equilibrium noise may thus become larger or smaller than the noise at $V = 0$. Concrete results are shown in Fig. 4, where the finite frequency excess noise is plotted as a function of the applied voltage bias V and the magnetic flux ϕ . Regions of negative excess noise are present, and can be reached simply by varying ϕ . Fig. 5 describes the same effect, yet, as a function of the side gate voltage V_G . These results show that in an Aharonov-Bohm interferometer the sign of the excess noise can be tuned either magnetically or electrostatically.

To conclude, we wish to shortly discuss the order of

magnitude of the parameters involved. Experimental evidence for Aharonov-Bohm oscillations has been found in semiconductor-based rings in the mesoscopic regime^{36–41} and, quite recently, in graphene-based rings⁴² in the mesoscopic regime. With respect to metallic rings, semi-conducting structures offer the advantage of exhibiting a dependence on the side gate voltage, thus being electrostatically tunable in the same way as discussed in our model. The typical size L of such rings is about $1\mu\text{m}$, which corresponds to an energy E_L of about 1meV , or equivalently to a ballistic frequency E_L/\hbar of about 1THz . Although this frequency regime was far from experimental reach two decades ago, more recent high frequency measurements^{9,14} show that nowadays the THz

range is no longer unrealistic. It thus seems likely that our proposal for tuning the sign of the excess noise can be tested in the near future.

IV. ACKNOWLEDGEMENTS

One of the authors (H.G.) wishes to thank Peter Hänggi for a stimulating cooperation during the days when we both moved as young researchers between Stuttgart, Basel, Philadelphia, New York, San Diego, Rehovot, and elsewhere. The authors acknowledge support by the Excellence Initiative of the German Federal and State Governments.

-
- * fabrizio.dolcini@polito.it
- ¹ S. Kogan, *Electronic Noise and Fluctuations in Solids* (Cambridge University Press, 1996).
 - ² Y. M. Blanter and M. Büttiker, *Phys. Rep.* **336**, 1 (2000).
 - ³ C. Beenakker and C. Schönberger, *Physics Today* **56**, 37 (2003).
 - ⁴ R. dePiccioto *et al.*, *Nature (London)* **389**, 162 (1997).
 - ⁵ L. Saminadayar *et al.*, *Phys. Rev. Lett.* **79**, 2526 (1997).
 - ⁶ F. Elste, S. M. Girvin, and A. A. Clerk, *Phys. Rev. Lett.* **102**, 207209 (2009).
 - ⁷ F. Elste, S. M. Girvin, and A. A. Clerk, *Phys. Rev. Lett.* **103**, 149902 (2009).
 - ⁸ G.B. Lesovik, and R. Loosen, *JETP Lett.* **65**, 295 (1997).
 - ⁹ R. Aguado and L.P. Kouwenhoven, *Phys. Rev. Lett.* **84**, 1986 (2000).
 - ¹⁰ U. Gavish, Y. Levinson, and Y. Imry, *Phys. Rev. B* **62**, 10637 (2000).
 - ¹¹ A.A. Clerk, M.H. Devoret, S.M. Girvin, F. Marquardt, and R.J. Schoelkopf, *Introduction to Quantum Noise, Measurement and Amplification*, arXiv:0810.4729.
 - ¹² M. B. Johnson, *Phys. Rev.* **29**, 367 (1927).
 - ¹³ H. Nyquist, *Phys. Rev.* **32**, 110 (1928).
 - ¹⁴ R. Deblock, E. Onac, L. Gurevich, and L. P. Kouwenhoven, *Science* **301**, 203 (2003).
 - ¹⁵ R. J. Schoelkopf, P. Wahlgren, A. A. Kozhevnikov, P. Delsing, D. E. Prober, *Science* **280**, 1238 (1998).
 - ¹⁶ M. Büttiker, *Phys. Rev. B* **45**, 3807 (1992).
 - ¹⁷ W. Schottky, *Ann. Phys. (Leipzig)* **57**, 541 (1918).
 - ¹⁸ A. Kumar, L. Saminadayar, D. C. Glattli, Y. Jin, and B. etienne, *Phys. Rev. Lett.* **76**, 2778 (1996).
 - ¹⁹ U. Gavish, Y. Levinson, and Y. Imry, *Phys. Rev. Lett.* **87**, 216807 (2001).
 - ²⁰ M. Reznikov, M. Heiblum, H. Shtrikman, and D. Mahalu, *Phys. Rev. Lett.* **75**, 3340 (1995).
 - ²¹ G. B. Lesovik and R. Loosen, *Z. Phys. B* **91**, 531 (1993).
 - ²² F. Dolcini, B. Trauzettel, I. Safi, and H. Grabert, *Phys. Rev. B* **75**, 045332 (2007).
 - ²³ M. Büttiker, Y. Imry, M. Ya. Azbel, *Phys. Rev. A* **30**, 1982 (1984).
 - ²⁴ M. Büttiker, *Phys. Rev. B* **32**, 1846 (1985).
 - ²⁵ G. Kurizki, *Phys. Rev. Lett.* **66**, 2609 (1991).
 - ²⁶ G.B. Lesovik and L.S. Levitov, *Phys. Rev. Lett.* **72**, 538 (1994).
 - ²⁷ F. Marquardt and C. Bruder, *Phys. Rev. B* **65**, 125315 (2002).
 - ²⁸ F. Dolcini and F. Giazotto, *Phys. Rev. B* **75**, 140511 (2007).
 - ²⁹ M. A. Davidovich, E. V. Anda, *Phys. Rev. B* **50**, 15453 (1994).
 - ³⁰ G.-B. Zhang, S.-J. Wang, and L. Li, *Phys. Rev. B* **74**, 085106 (2006).
 - ³¹ T.-F. Fang, S.-J. Wang, and W. Zuo, *Phys. Rev. B* **76**, 205312 (2007).
 - ³² M. Büttiker, *J. Phys. Cond. Matt.* **5**, 9361 (1993).
 - ³³ M. Büttiker, *J. Math. Phys.* **37**, 4793 (1996).
 - ³⁴ A. Prêtre, H. Thomas, and M. Büttiker, *Phys. Rev. B* **54**, 8130 (1996).
 - ³⁵ I. Safi, arXiv: 0908.4382 and arXiv:0906.4658.
 - ³⁶ G. Timp *et al.*, *Phys. Rev. Lett.* **58**, 2814 (1987).
 - ³⁷ S. Pedersen *et al.*, *Phys. Rev. B* **61**, 5457 (2000).
 - ³⁸ A. Fuhrer *et al.*, *Nature* **413**, 822 (2001).
 - ³⁹ W. G. van der Wiel *et al.*, *Phys. Rev. B* **67**, 033307 (2003).
 - ⁴⁰ D. V. Nomokonov and A. A. Bykov, *JETP Lett.* **82**, 89 (2005).
 - ⁴¹ I. Neder, M. Heiblum, D. Mahalu and V. Umansky, *Phys. Rev. Lett.* **98**, 036803 (2007).
 - ⁴² S. Russo *et al.*, *Phys. Rev. B* **77**, 085413 (2008).